Exploration Geophysics, Remote Sensing and Environment XXVII.2 (2020)

DOI: 10.26345/EGRSE-033-20-203

SPATIAL-TEMPORAL CHANGES OF LAND SURFACE TEMPERATURE IN DEPENDENCE ON LAND COVER, ALTITUDE AND NDVI IN SELECTED AREAS OF CZECHIA

PROSTOROVÉ ZMĚNY POVRCHOVÝCH TEPLOT V ČASE V ZÁVISLOSTI NA KRAJINNÉM POKRYVU, NADMOŘSKÉ VÝŠCE A NDVI NA VYBRANÝCH ÚZEMÍCH ČESKÉ REPUBLIKY

Martin Hofrajtr [1], Jana Seidlová [2], Iva Batrlová [3], Jiří Kvapil [4], Pavel Doubrava [5]

Abstract

Land surface temperature and its study is an important part of evaluating the energy balance of the upper part of the Earth's surface. Nowadays, the problem of overheating of the Earth's surface in cities is often discussed, where this phenomenon consequently significantly affects the local climate and thus the health of people living there. The paper deals with the analysis of land surface temperature from Landsat 8 satellite infrared thermal data across urban and rural areas in Czechia. Results of the dependence of the land surface temperature on the normalized differential vegetation index (NDVI) and altitude in two intersecting areas of interest show that people living in an open agricultural landscape may be exposed to higher temperatures during the period of dormancy. Bare arable land has similar thermal properties to urban surfaces and, due to increased absorption of solar energy, can at certain times of the year reach even higher average temperatures than urban surfaces and negatively affect their surroundings. Therefore, land surface temperature must be seen as a distinctly spatially and temporally dynamic phenomenon. By taking appropriate environmental measures in places with higher surface temperatures, overheating of the Earth's surface due to climate change could be prevented in the future.

Abstrakt

Povrchová teplota a její studium je důležitou součástí vyhodnocování energetické bilance svrchní části zemského povrchu. V dnešních dnech je často diskutována problematika přehřívání zemského povrchu ve městech, kde je tímto fenoménem následně výrazně negativně ovlivňováno lokální klima, a tedy i zdraví lidí zde žijících. Článek se zabývá analýzou povrchových teplot z družicových infračervených termálních dat napříč městskými i rurálními oblastmi na území České republiky. Z výsledků závislosti povrchové teploty na

normalizovaném diferenčním vegetačním indexu (NDVI) vyplývá, že v době vegetačního klidu mohou být vyššími teplotami ohroženi i lidé žijící v otevřené zemědělské krajině. Holé orné půdy mají podobné tepelné vlastnosti jako městské povrchy a kvůli zvýšené absorpci sluneční energie mohou v určitých částech roku dosahovat i vyšších průměrných teplot než zmíněné městské povrchy a negativně ovlivňovat své okolí. Proto je nutné na povrchové teploty nahlížet jako na výrazně prostorově a časově dynamický jev.

Keywords

altitude, land cover, land surface temperature, NDVI

Klíčová slova

nadmořská výška, krajinný pokryv, povrchová teplota, NDVI

1. INTRODUCTION

Currently, the problem of overheating of the Earth's surface is often discussed in connection with climate change and warming. The main cause of this phenomenon is the change of the active part of the surface due to anthropogenic activities (Středová et al., 2010). In particular urban-type surfaces such as asphalt and concrete are considered to have a tendency to overheat and so studies focus primarily on large agglomerations (Arnds et al., 2017; Zhou et al., 2017). This phenomenon is known as so-called urban heat island, which is characterized by higher air and surface temperatures compared to the surrounding rural landscape (Oke, 1973; Středa et al., 2011).

In Czechia, the effect of the urban heat island was monitored in large cities, e.g. Prague and Brno, mainly based on ground air temperature data from meteorological stations (Dobrovolný et Krahula, 2015). Ground air temperature monitoring can be complemented by land surface temperature (LST) data obtained by remote sensing infrared thermal data. Thanks to continuous data from the whole area of interest and relatively short interval between two consecutive measurements (1 – 2 times a month) local or global changes can be monitored in smaller detail.

This article aims to analyse the spatial distribution of LST during one year in Czechia and to study its dependence on selected aspects – land cover, altitude and normalized differential vegetation index (NDVI). Partial goal of this article will be comparison of surface temperature results in individual types of land coverage – urban areas and agricultural landscapes.

2. AREAS OF INTEREST

The results of the LST analysis relate to two areas of interest consisting of the intersection of scenes 190–026 and 191–025 of the World Reference System (WRS) with the territory of Czechia, see Fig. 1. In Czechia, scene 191–025 (area A) covers central, north and eastern part of Bohemia with the area of 27,165 km^2. Scene 190–026 (area B) covers part of southern Moravia and southeast Bohemia with the total area of 17,100 km^2. These areas have been chosen both for their diverse land cover and relatively high altitudinal heterogeneity, as well as for the relatively good availability of high-quality Landsat 8 satellite data with low or no cloud cover.

Areas A and B consist mainly of agricultural areas (60.6% and 63.9%), forests and semi-natural areas (31.1% and 28.9% respectively) account for a large part, while urbanized areas occupy 7.8%, and 6.5% respectively, water bodies and so-called humid areas occupy only a negligible part of the total area of interest (CENIA, 2018). Regarding altitudinal heterogeneity, most of the two areas of interest acquire altitudes from 200 to 500 m above sea level.

It is important to add that the results of the analysis always relate to only one of the areas of interest, i.e. only area A or area B. The overlapping part of these areas is therefore evaluated separately for each area of interest.

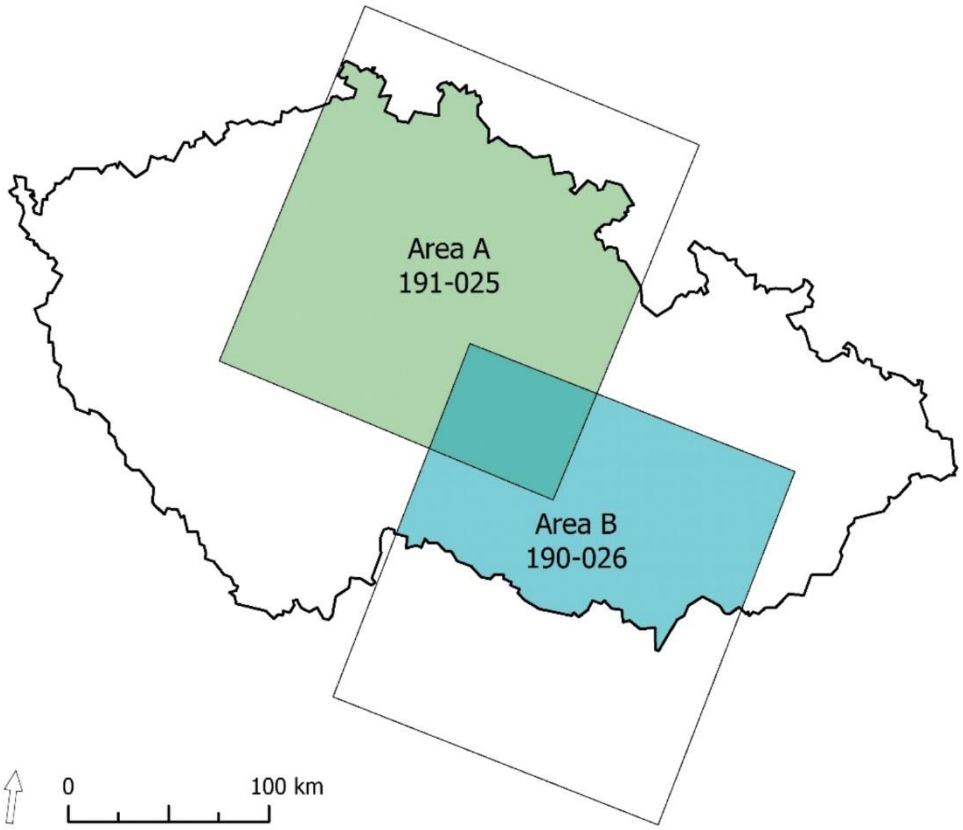

Fig. 1 Areas of interest consisting of the intersection of scenes 190-026 and 191-025 within the territory of Czechia

3. MATERIAL AND METHODS

Landsat 8 satellite data were used to calculate the LST in the areas of interest. This satellite carries two sensors – OLI (Operational Land Imager) and TIRS (Thermal Infrared Sensor) (Montanaro et al., 2014).

The WRS is used to store images taken by Landsat 8. For analyses in this paper images from scenes 191–025 and 190–026 were used. Specifically, the images from 1st April, 19th May, 20th June, 7th August of 2017 from scene 191–025, and those from 19th April, 31st May, 19th August, 20th August, and 6th October of 2018 from scene 190–026.

Values of spectral radiance are influenced by the passage of radiation through the atmosphere, namely the attenuation and back reflection of the Earth's surface radiation and the atmospheric radiation itself (Howell et al. 2015). In order to eliminate these effects, values of spectral radiance in the upper atmosphere layer (L_{TOA}) were atmospherically corrected to values of spectral radiance values leaving the Earth's surface (L_T), see Eq. 1, so-called radiation transfer equation (Muňoz et Sobrino, 2006).

$$L_T = \frac{L_{TOA} - (1-\varepsilon)\cdot L^{\downarrow}_{atm} - L^{\uparrow}_{atm}}{\varepsilon\tau} \quad (1)$$

where ε expresses the emissivity of the Earth's surface, τ transmissivity of the atmosphere, $L^{\downarrow}_{atm}$ backscattered radiation of the Earth's surface, $L^{\uparrow}_{atm}$ direct radiation of the atmosphere. The web application Atmospheric Correction Parameter Calculator (Barsi et al., 2003, 2005) was used to calculate the values of transmissivity, backscattered radiation of the Earth's surface and direct spectral radiance of the

atmosphere. Values of spectral radiation leaving the Earth's surface L_T were subsequently converted to a brightness temperature T_R, see Eq. 2 (USGS 2018).

$$\boldsymbol{T_R = \frac{K_2}{\ln\left(\frac{K_1}{L_T}+1\right)}} \tag{2}$$

where k_1 is the first TIRS sensor band 10 temperature constant of 774.8853 nm and k_2 is the second TIRS sensor band 10 temperature constant of 1321.0778 nm. The knowledge of land surface emissivity is required to convert surface temperature brightness to thermodynamic surface temperature. There are several options for determining emissivity, for the purpose of this paper the method by (Sobrino et al., 2004) was used – emissivity thresholding from the NDVI, which can be calculated from processed satellite data based on the knowledge of the reflectance of the red R and near infrared band NIR, see Eq. 3.

$$\boldsymbol{NDVI = \frac{NIR-R}{NIR+R}} \tag{3}$$

In this method, three types of land cover are distinguished by NDVI – bare soil (NDVI < 0.2), mixed cover (0.2 ≤ NDVI ≤ 0.5) and vegetation (NDVI > 0.5). If the land cover is determined as bare soil or vegetation, it is assigned a constant emissivity value of 0.973 and 0.990 respectively (average emissivity values calculated by the authors of the method based on data from the ASTER spectral library). In the case of mixed cover, the emissivity is calculated based on Eq. 4.

$$\boldsymbol{\varepsilon = 0,004 \cdot P_V + 0,986} \tag{4}$$

where P_V expresses the vegetation ratio based on Eq. 5.

$$\boldsymbol{P_V = \left(\frac{NDVI - NDVI_{min}}{NDVI_{max} - NDVI_{min}}\right)^2} \tag{5}$$

where NDVI expresses the value of normalized differential vegetation index, $NDVI_{min}$ and $NDVI_{max}$ thresholds distinguishing between mixed cover and vegetation respectively bare soils, i.e. 0.2 and 0.5. The thermodynamic LST T_T was calculated from the values of the brightness surface temperature T_R and the land surface emissivity ε, see Eq. 6, which is based on the inversion of the Planck radiation law (Artis et Carnahan, 1982).

$$\boldsymbol{T_T = \frac{T_R}{1+\frac{\lambda \cdot T_R}{\left(\frac{h \cdot c}{k}\right)} \ln \varepsilon}} \tag{6}$$

where λ [m] represents the wavelength of a given band and sensor, h Planck's constant 6.626,070,040 × 10^{-34} J · s, k a Boltzmann's constant of 1.380,648,520 × 10^{-23} J · K^{-1} and c a light speed of 2.997,924,58 × 10^8 m · s^{-1} in vacuum. For the resulting LST to be in degrees Celsius, Eq. 6 had to be supplemented by a deduction of value 273.15, which corresponds to an absolute zero in the Celsius temperature scale.

LST were rounded to the next higher value to optimize comparisons. NDVI raster data were merged to 11 classes to optimize comparison with other layers.

In addition to satellite data, data from the CORINE Land Cover (CLC) database (CENIA, 2018) from 2018 and the digital elevation model data (ArcČR, 2019) from 2010 were also used. CLC vector data has been modified to optimize comparison with other layers. This vector layer was then resampled to a 30 m pixel raster. The DEM raster layer was resampled to a pixel size of 30 m. To optimize comparison with other layers, the layer was merged into 15 classes according to altitude at intervals of one hundred meters. All raster images were projected to UTM Zone 33 N in the WGS 1984 system.

4. RESULTS

The graphical output of the analysis herein applies, except for the surface temperature-altitude profile, solely on 31st May and 6th October for Scene 190–026 and 19th May and 7th August for Scene 191–025. This step was made because of the clear spatial variation of LST between these acquisition times. However, results in the text form also contain information about the analysed data from other acquisition times. For the sake of clarity, results related to individual relationships are divided into the following three subchapters.

4.1 Relationship between LST and land cover

The analysis of LST within individual classes of land cover revealed that during the growing season they reached the highest average temperatures at the built-up area (28.63 °C in area A and 29.60 °C in area B, respectively). At that time, agricultural areas are largely covered by growing vegetation and their temperature is on average almost 3.0 °C and 2.5 °C lower. An interesting indicator for agricultural areas is the standard deviation of LST values from the average, which in both areas of interest reaches the highest values compared to the other classes (2.35 and 3.19). Such high values indicate the proportion of agricultural areas covered by vegetation and those without vegetation. The difference in average LST between built-up and agricultural areas varies considerably during that part of the year when the fields are harvested. This results in an alignment of temperature averages between these areas or even higher average LST in agricultural areas (Area A), see Table 1a and Table 1b. In the spring

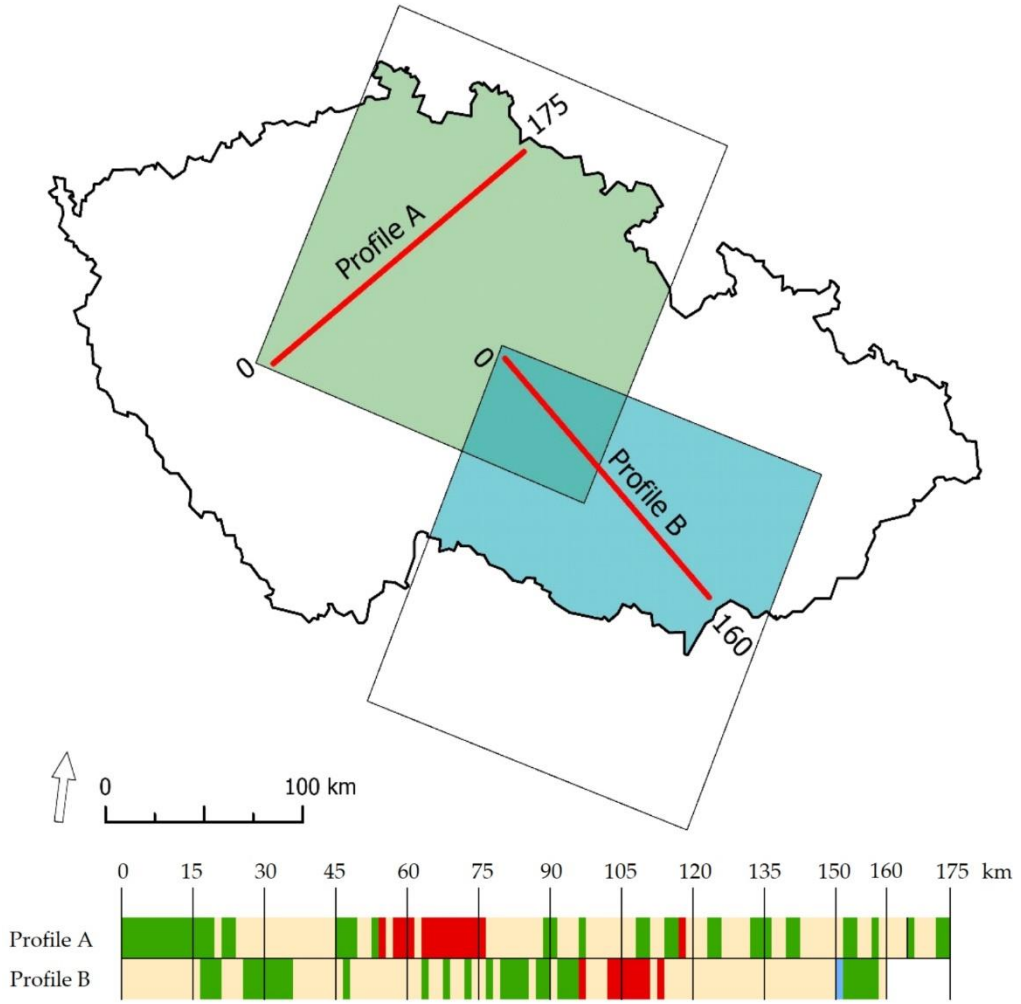

Fig. 2 Profiles A and B within the First and Second area of interest (top) and representation of the CORINE Land Cover classes in their course

months, cities of Prague and Brno are clearly visible in areas A and B (shown in light yellow to white), which emit much more energy than the surrounding landscape, acquire higher LST and form urban heat islands. However, this phenomenon is no longer noticeable in October months, when on harvested bare arable land they sometimes reach the same or even higher temperatures than urban surfaces.

Table 1a Average LST and their standard deviations in each class of CORINE Land Cover in area A

	19th May			**7th August**		
	Area [km²]	**LST [$\bar{x}$]**	**LST [σ]**	**Area [km²]**	**LST [$\bar{x}$]**	**LST [σ]**
Artificial surfaces	2 117.54	28.63	2.35	1 831.45	27.79	2.68
Agricultural areas	16 450.14	25.60	2.77	14 010.13	26.66	3.74
Forest and seminatural areas	8 429.79	23.90	1.73	6 572.71	21.52	2.05
Wetlands	7.02	25.15	1.73	5.60	22.68	1.62
Water bodies	143.98	22.58	2.12	129.68	23.82	1.57

Table 1b Average LST and their standard deviations in each class of CORINE Land Cover in area B

	31st May			**6th October**		
	Area [km²]	**LST [$\bar{x}$]**	**LST [σ]**	**Area [km²]**	**LST [$\bar{x}$]**	**LST [σ]**
Artificial surfaces	984.98	29.60	2.55	928.15	15.68	1.90
Agricultural areas	9 302.27	27.07	3.19	9 971.39	16.05	2.67
Forest and seminatural areas	4 149.81	24.21	2.33	4 480.24	12.74	2.09
Wetlands	6.04	25.27	1.93	6.04	16.66	1.54
Water bodies	92.92	23.20	1.84	103.30	13.75	1.90

4.2 Relationship between LST and altitude

In order to compare LST and altitude, profiles A and B were created, intersecting both areas of interest. In area A, the profile length was 175 km and led from Brdské Hřebeny, across Prague, south of Mladá Boleslav to the western part of the Giant Mountains; in area B the profile length was 160 km and led from the upper left corner of the scene across Brno to the border with Slovakia, see Fig. 2. The lower part of the picture shows the most represented land cover class in the given profile – agricultural areas and forests, the red parts are made up of the cities of Prague (Profile A) and Brno (Profile B). Graphically expressed values of surface temperatures, altitude and NDVI in the graphs always refer to the whole intervals of 1.5 km, in which the values from individual pixels were averaged.

Fig. 3 (a) and (b) shows the dependence of LST on altitude (grey colour) within the temperature profile. With increasing altitude, LST generally decrease. This fact can also be supported by the high negative correlation found between these two variables, see Table 2a and 2b. The correlation coefficient in the area B reached values around -0.90 in all analysed months. For the area A, such high correlation coefficients were found only in April and May, in the summer months this dependence was significantly lower (approx. -0.73 and -0.79).

Table 2a Correlation coefficients indicating a negative correlation between LST and altitude in area A

1st April	19th May	20th June	7th August
-0.93005	-0.91752	-0.73444	-0.78685

Table 2b Correlation coefficients indicating a negative correlation between LST and altitude in area B

29th April	31st May	19th August	20th September	6th October
-0.90676	-0.90141	-0.90626	-0.89089	-0.94136

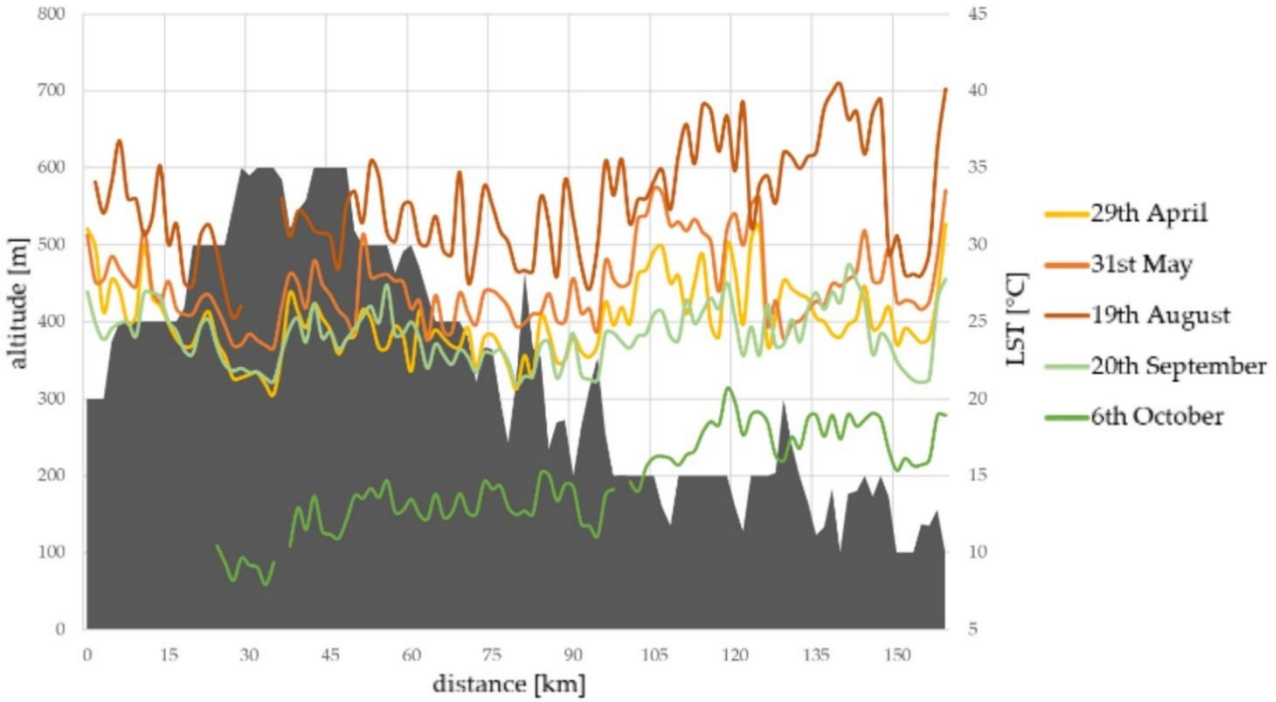

Fig. 3a Profile A showing dependence between LST and altitude

4.3 Relationship between LST and NDVI

Same profiles A and B were used to analyse the dependence between LST and NDVI. Fig. 4 shows this dependence in area A – a large decrease in NDVI in the 60–75 km section is caused by the Prague agglomeration, in other cases (especially in the August image) the low NDVI corresponds to harvested or already ploughed arable land within agricultural areas (especially the area between Prague and the foothills of the Giant Mountains).

Similarly, in Area B, see Fig. 5, where the large decrease in NDVI over the 100–110 km section is due to the Brno agglomeration. The southern part of Moravia is one of the warmest areas of Czechia (ČHMÚ, 2019) and it is also an area that, thanks to high-quality soil (MŽP 2019), provides ideal conditions for agriculture. As in Area A, there is a noticeable local decline in NDVI in late summer. This is caused by areas of bare soil without vegetation in areas where crops have already been harvested. The absence of vegetation is also associated with a direct influence of the Earth's surface by solar radiation – it can absorb much larger amounts of thermal energy and thus acquires much higher LST. An exemplary map result from surface temperatures and NDVI in area A (19th May 2018) is displayed in Fig. 6.

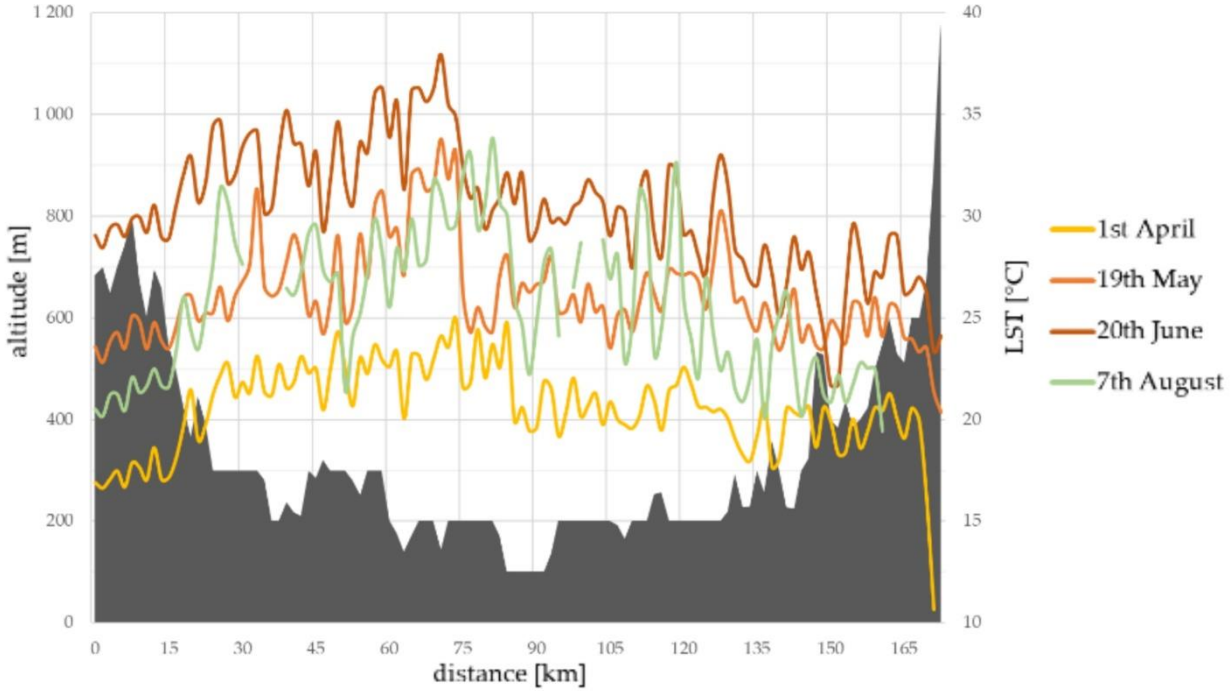

Fig. 3b Profile B showing dependence between LST and altitude

As in the previous case, correlation was used to quantify the dependence of these two variables. Table 3a and 3b contains a pair of values, in the first row the values correspond to the correlation coefficient found from the whole area, in the second row the correlation coefficients

Table 3a Correlation coefficients indicating a negative correlation between LST and altitude in area A

	1st April	19th May	20th June	7th August
all pixels	0.45635	0.16725	0.22642	-0.11419
pixels with NDVI value >= 0,3	-0.91106	-0.97001	-0.97585	-0.98472

were calculated only for NDVI values higher than 0.3. In the case of filtered pixels with low NDVI, the correlation coefficient ranged from -0.91 to -0.98 – a very strong negative correlation. In area B, the correlation coefficient values were more dispersed and at the same time more different between the two subsequent periods, but the negative correlation can still be determined as very strong.

Table 3b Correlation coefficients indicating a negative correlation between LST and altitude in area B

	29th April	**31st May**	**19th August**	**20th September**	**6th October**
all pixels	0.21943	0.22083	-0.27511	0.21673	-0.35419
pixels with NDVI value >= 0,3	-0.81668	-0.95500	-0.79941	-0.94224	-0.76034

5. DISCUSSION

The paper describes and compares the spatial distribution of LST and its changes in dependence on land cover, altitude and NDVI during 2017 and 2018 in selected areas of interest in Czechia. Landsat 8 infrared thermal satellite data with high spatial resolution were used for this purpose.

The analysis of these data showed that the distribution of LST during the year is a very dynamic phenomenon – cities accumulate and emit more energy than the surrounding landscape, especially during the growing season, while in the time of dormancy this state changes and the surrounding landscape's LST is on average similar to urban areas. With regard to the fact that approximately 53.3% of the area of Czechia (ČÚZK, 2019) is occupied by agricultural areas (built-up areas represent only 1.68%), 70.4% of which is arable land, overheating of areas in this part of the landscape is a more serious problem – the effect on air temperature increase, rapid water discharge, increased evaporation and consequent drought risk. The trend of decreasing LST with increasing altitude was also confirmed; this phenomenon is largely associated with similar air temperature behaviour. A very strong correlation was found between the NDVI and the surface temperature – except for two periods, the correlation coefficient value was less than -0.81, indicating a very high relationship (negative correlation) between the two variables.

The question is to what extent it is possible to talk about the effect of the so-called urban heat island of the city. Although, for instance, Dobrovolný (2012) using the example of the city of Brno, speaks of this phenomenon, the map results show high LST values in agricultural landscape areas. The urban heat island of the city was also mentioned by Sedlák et al. (2010) in case of studying the LST of Olomouc and its surroundings, even though data from only one day were evaluated. The evaluation of the LST characteristics and its behaviour on the basis of such a limited number of data is insufficient. However, this work also had a limited number of satellite images from the areas of interest – the temporal resolution and occurrence of clouds in the images significantly reduce the usability of available Landsat data. Nevertheless, it can be stated that rather than the urban effect, it is a nationwide effect caused by uncontrolled anthropogenic activity not only in urban areas but also in their surroundings.

a)

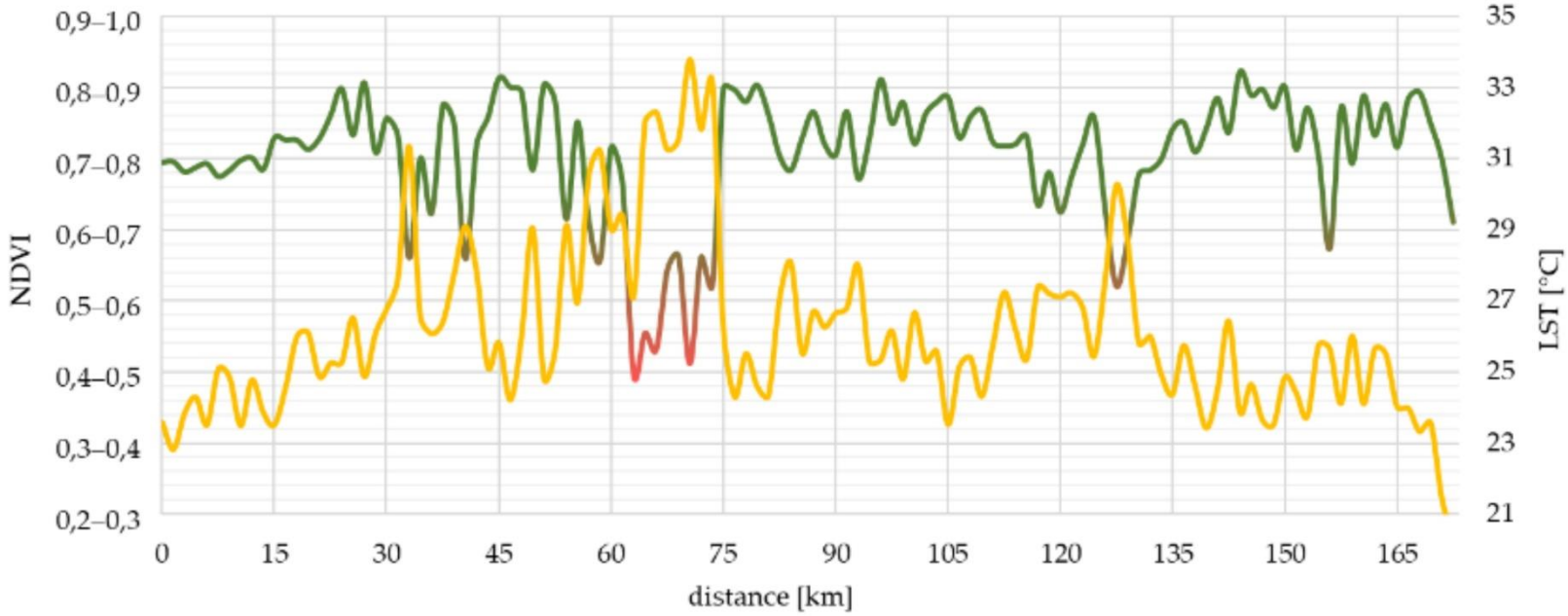

b)

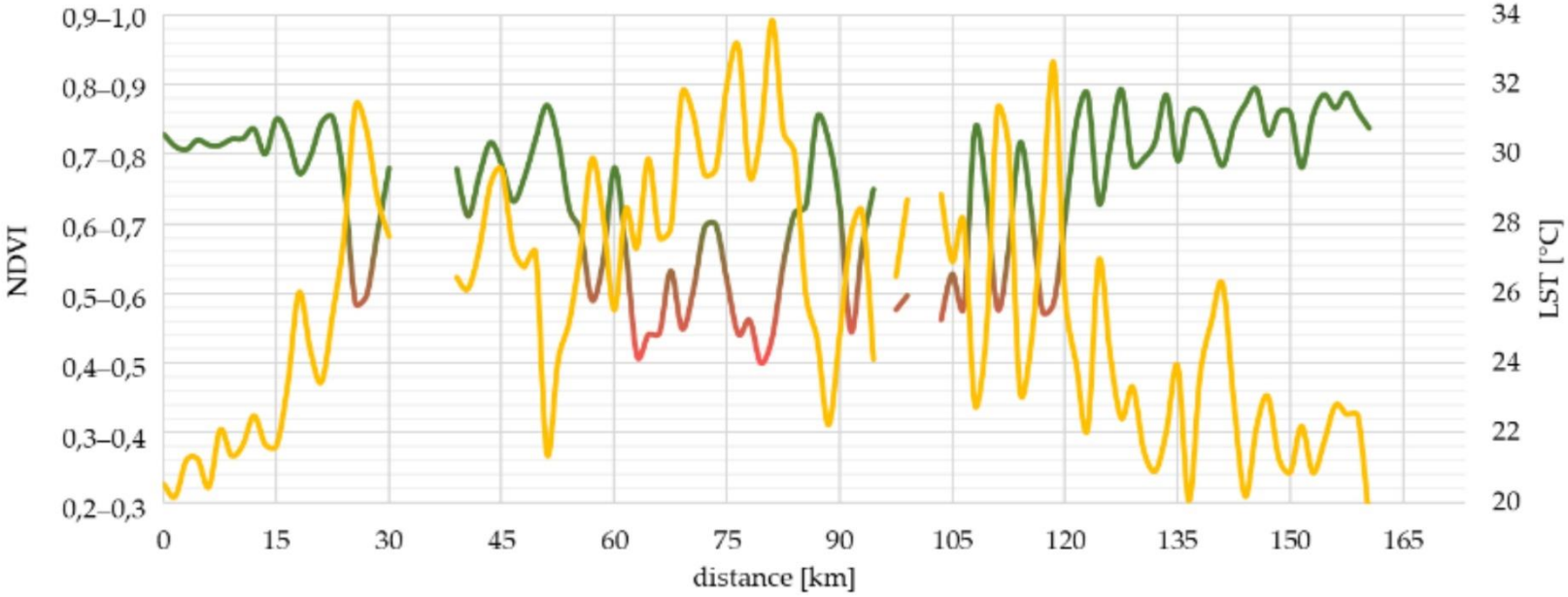

Fig. 4 Profile A showing dependence between LST – yellow curve and NDVI – red-green curve (19th May 2017 (a) and 7th August 2017 (b))

a)

b)

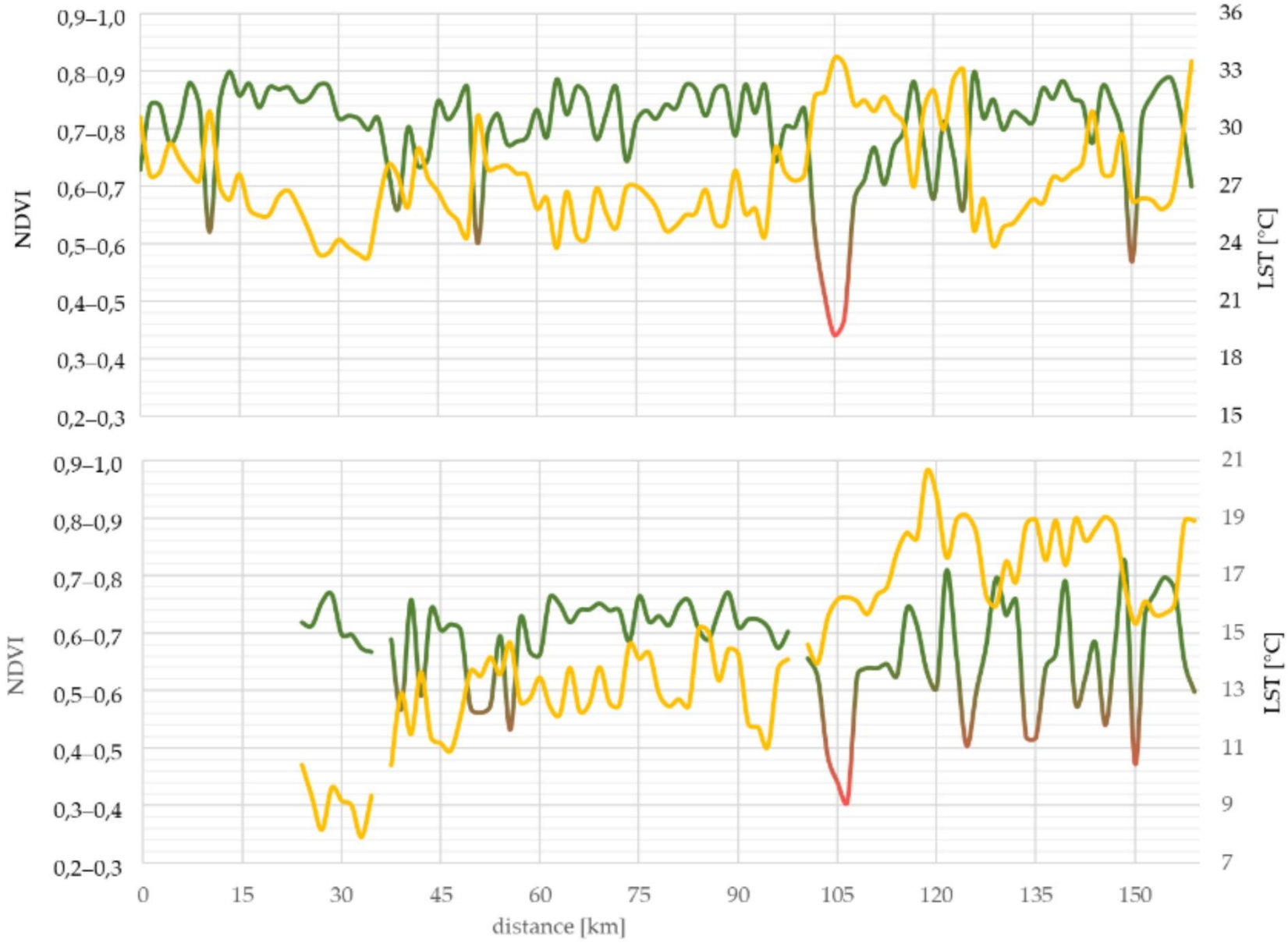

Fig. 5 Profile B showing dependence between LST – yellow curve and NDVI value – red-green curve (31st May 2018 (a) and 6th October 2018 (b))

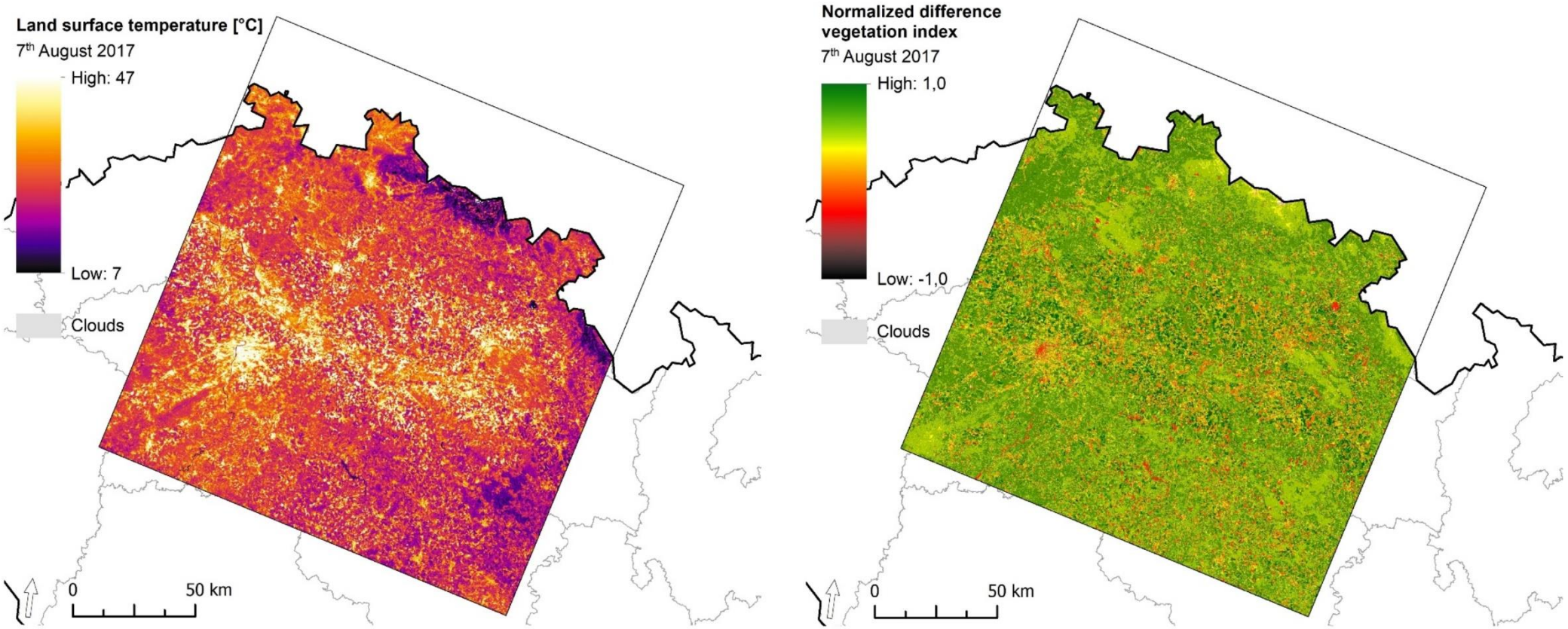

Fig. 6 Map of LST (a) and NDVI (b) in area A (19th May 2018)

6. CONCLUSION

The article dealt with spatial changes in LST during a year in two areas of interest in Czechia. In the case of agricultural areas, significant differences in LST from built-up areas are only observed at the beginning of the growing season. During the year the LST of agricultural areas and buildings are very similar. This fact was supported by statistical and map outputs. The NDVI achieved a very strong correlation with the LST (when water was filtered out), which clearly showed the influence of the vegetation cover on the LST.

References:

ARNDS, D., BÖHNER, J., BECHTEL, B. Spatio-temporal variance and meteorological drivers of the urban heat island in a European city. *Theoretical and Applied Climatology*, 2017, 128: p. 43–61.

ARTIS, D., A., CARNAHAN, W., H. Survey of emissivity variability in thermography of urban areas. *Remote Sensing of Environment*, 1982, 12: p. 313–329.

BARSI, J., A., BARKER, J., L., SCHOTT, J., R. An atmospheric correction parameter calculator for a single thermal band earth-sensing instrument. *IEEE International Geoscience and Remote Sensing Symposium*, 2003.

BARSI, J.A., SCHOTT, J.R., PALLUCONI, F.D., HOOK, S.J. Validation of a web-based atmospheric correction tool for single thermal band instruments. *Earth Observing Systems X*, 2005, 5882: 7.

DOBROVOLNÝ, P. The surface urban heat island in the city of Brno (Czech Republic) derived from land surface temperatures and selected reasons for its spatial variability. *Theoretical and Applied Climatology*, 2012, p. 200.

DOBROVOLNÝ, P., KRAHULA, L. The spatial variability of air temperature and nocturnal urban heat island intensity in the city of Brno, Czech Republic. *Moravian Geographical Reports*, 2015, 23: p. 8–16.

HOWELL, R., MENGUC, M.P., SIEGEL, R. *Thermal radiation heat transfer*. CRC Press, Boca Raton, 2015, p. 1016.

MONTANARO, M., GERACE, A., et al. Stray light artifacts in imagery from the Landsat 8 Thermal Infrared Sensor. *Remote Sensing*, 2014, 6: p. 10435–10456.

OKE, T.R. City size and the urban heat island. *Atmospheric Environment Pergamon Press*, 1973, 7: p. 769–779.

SEDLÁK, P., PRISLINGER, J., VYSOUDIL, M. Využití dat z družice LANDSAT pro detekci tepelného znečištění v městské a příměstské krajině. *Scientific Papers of the University of Pardubice - Series D*: Faculty of Economics and Administration, 2010, p. 264–278.

STŘEDA, T., POKLADNÍKOVÁ, H., FUKALOVÁ, P., ROŽNOVSKÝ, J. Temperature conditions of Brno city on the level of mezoclimate and microclimate. *Práce Geograficzne*, 2011, p. 19–27.

STŘEDOVÁ, H., FUKALOVÁ, P., ROŽNOVSKÝ, J. Specifics of temperature extremes in the conditions of the urban climate. *Contributions to Geophysics & Geodesy*, 2010, p. 249–261.

SOBRINO, J.A., JIMENEZ-MUŇOZ, J.C., PAOLINI, L. Land surface temperature retrieval from Landsat TM 5. *Remote Sensing of Environment*, 2004, 90: p. 434–440.

USGS *Landsat 8 Data users handbook*. EROS, 2018, p. 115.

ZHOU, B., RYBSKI, D., KROPP, J.P. The role of city size and urban form in the surface urban heat island. *Scientific Reports*, 2017, 7: p. 1–7.

CENIA *CORINE Land Cover 2018 database of the Czech Republic*. https://land.copernicus.eu/pan-european/corine-land-cover, 2018.

ČHMÚ *Climate characteristics maps*. http://portal.chmi.cz/historicka-data/pocasi/mapy-charakteristik-klimatu, 2019.

ČÚZK *Summary overviews of the land fund from the data of the Real Estate Cadastre of the Czechia*. https://www.cuzk.cz/Periodika-a-publikace/Statisticke-udaje/Souhrne-prehledy-pudniho-fondu/Rocenka_pudniho_fondu_2019.aspx, 2019.
MŽP *Soil maps*. https://www.mzp.cz/cz/pudni_mapy, 2019.

Authors:
[1] Mgr. Martin Hofrajtr, CENIA, Prague, Czech Republic; Vršovická 1442/65, 100 10 Praha 10-Vršovice, martin.hofrajtr@cenia.cz
[2] Ing. Jana Seidlová, CENIA, Prague, Czech Republic; Vršovická 1442/65, 100 10 Praha 10-Vršovice, jana.seidlova@cenia.cz
[3] Ing. Iva Batrlová, CENIA, Prague, Czech Republic; Vršovická 1442/65, 100 10 Praha 10-Vršovice, iva.batrlova@cenia.cz
[4] Mgr. Jiří Kvapil, CENIA, Prague, Czech Republic; Vršovická 1442/65, 100 10 Praha 10-Vršovice, jiri.kvapil@cenia.cz
[5] RNDr. Pavel Doubrava CENIA, Prague, Czech Republic; Vršovická 1442/65, 100 10 Praha 10-Vršovice, pavel.doubrava@cenia.cz